2) At a fixed inlet temperature and pressure the CV with the bigger throat diameter will have a higher rechoked pressure-difference ratio because of the lower loss coefficient.

3) If overflow is induced in CVs, Eq. (6) would permit an estimate of the pressure-difference ratio at cavitation inception.

4) According to the comparison of the test results and the analysis, the pressure-difference ratio at rechoking can be reasonably predicted using Eq. (6) at a given loss coefficient and inlet subcooling using the superheat that was found experimentally.

Acknowledgments

The authors wish to acknowledge the support provided by the National Science Committee, Taiwan, Republic of China, Research Grant NSC 86-2221-E-224-020, for making this study possible. They also acknowledge the invaluable assistance of E. K. Ungar at NASA Johnson Space Center.

References

[1]Hamitt, F. G., Ahmed, O. S. M., and Hwang, J.-B., "Performance of Cavitating Venturi Depending on Geometry and Flow Parameters," *Proceedings of the ASME Cavitation and Polyphase Flow Forum*, American Society of Mechanical Engineers, New York, 1976, pp. 18–21.

[2]Ungar, E. K., Dzenitis, J. M., and Sifuentes, R. T., "Cavitating Venturi Performance at Low Inlet Subcooling: Normal Operation, Overflow and Recovery from Overflow," *ASME Symposium on Cavitation and Gas-Liquid Flows in Fluid Machinery Devices*, FED-Vol. 190, American Society of Mechanical Engineers, New York, 1994, pp. 309–318.

[3]Hsu, Y. Y., "On the Size and Range of Active Nucleation Cavities on a Heating Surface," *Journal of Heat Transfer*, Vol. 84, No. 1, 1962, pp. 207–216.

[4]Avallone, E. A., and T. Baumeister, T., III, *Mark's Standard Handbook for Mechanical Engineers*, 9th ed., McGraw–Hill, New York, 1987.

[5]Liou, S. G., Chen, I. Y., and Sheu, J. S., "Testing and Evaluation of Small Cavitating Venturis with Water at Low Inlet Subcooling," *Proceedings of the Space Technology and Applications International Forum*, American Inst. of Physics, Woodbury, NY, 1998, pp. 479–487 (CP420).

Combined Conduction and Radiation Heat Transfer in a Cylindrical Medium

C. K. Krishnaprakas*
ISRO Satellite Centre, Bangalore 560 017, India

Nomenclature

$I_b(T)$ = blackbody radiation intensity, W/m^2-sr
$I(\tau, \hat{s})$ = radiation intensity at τ in the direction $\hat{s}$, W/m^2-sr
k = thermal conductivity of the medium, $k_0[1 + \alpha(T - T_1)]$, W/m-K
N_c = conduction–radiation number, $k_0\beta/4\sigma T_1^3$
$\hat{n}$ = normal vector to the surface
$p(\hat{s}, \hat{s}')$ = scattering phase function
$p(\mu_p)$ = single-scattering phase function
q = heat flux, W/m^2
r = radius of the cylinder, m
$\hat{s}$ = radiation direction vector
$\hat{s}_s$ = direction vector of the specularly reflected radiation from the boundary surface
T = temperature, K
α = coefficient for thermal conductivity variation, K^{-1}
β = extinction coefficient, $\kappa + \gamma$, m^{-1}
γ = scattering coefficient, m^{-1}
ε = emittance of boundary surface
η = direction cosine of $\hat{s}$ with the axis that is mutually orthogonal to the radius vector and the cylinder axis, $\sin\phi \sin\varphi$
θ = dimensionless temperature, T/T_1
κ = absorption coefficient, m^{-1}
μ = direction cosine of $\hat{s}$ with the radius vector, $\cos\phi \sin\varphi$
ν = variable thermal conductivity parameter, $k_0\alpha\beta/4\sigma T_1^2$
ρ = reflectance of the boundary surface, $\rho^d + \rho^s = 1 - \varepsilon$
ρ^d = diffuse reflectance of the boundary surface
ρ^s = specular reflectance of the boundary surface
σ = Stefan–Boltzmann constant, W/m^2-K^4
τ = optical depth of the medium at radius $r = \int_0^r \beta\, dr$
ϕ = angle between $\hat{s}$ and cylinder axis
ψ = azimuthal angle of $\hat{s}$ in the plane perpendicular to cylinder axis
Ω = solid angle, sr
ω = scattering albedo, γ/β

Subscript
1, 2 = boundary surfaces

Received Nov. 12, 1997; revision received March 11, 1998; accepted for publication May 4, 1998.

*Engineer, Thermal Systems Group.

Introduction

COMBINED conduction and radiation heat transfer in an absorbing, emitting, and scattering medium occurs in many engineering applications such as thermal insulation systems for cryogenic and space applications, propulsion systems, fluidized beds, optical engineering, solar engineering, nuclear engineering, atmospheric sciences, astrophysics, etc. Mathematical formulation of the problem leads to a complicated nonlinear integrodifferential system that is difficult to solve. In particular, coupled conduction and radiation heat transfer in planar systems has received the most attention by far, as reviewed by Viskanta[1] and Howell.[2] Relatively little work has been done for problems with cylindrical geometry despite their occurrence in many engineering applications. Fernandes and Francis[3] solved the coupled conduction and radiation problem for a gray absorbing, emitting, and isotropically scattering concentric cylindrical medium using a Galerkin finite element method. Pandey[4] solved the problem numerically using the undetermined parameters method, but did not consider scattering in the analysis. Harris[5] included anisotropic scattering in the analysis using the spherical harmonics method to solve the radiative transport equation.

The success of conduction/radiation analysis for cylindrical geometry depends to a large extent on the accurate modeling of the radiation field. Exact treatment of the radiative flux within a cylindrical medium is available for only very simple cases. To analyze a general problem, i.e., including anisotropic scattering, specular-diffuse boundaries, etc., alternate methods are to be resorted. Methods like Monte Carlo method or the Hottel's zone method, although accurate, require much computer time and storage and are not grid compatible with the other conservation equations. For higher-order approximations to the solution, the spherical harmonics method or the discrete ordinates method (also known as the S_N method) may be attempted.[6] Being differential in form, these methods are also grid compatible with the other conservation equations. Spherical harmonic methods involving complex mathematical manipulations and methods beyond P_3 makes the analysis too cumbersome. Compared to all of the other methods, the S_N

method seems to be a straightforward method to tackle problems of cylindrical geometry. Once the problem is formulated it is quite easy to switch over to higher-order S_N methods for better accuracy; the same is not the case with the P_N methods.

The dependence of thermal conductivity of the medium with temperature has not been investigated earlier in the analysis of combined conduction and radiation in cylindrical geometries. This is essential when large temperature differences exist across the medium. Also, the effect of specular reflection at the boundaries has also not been reported in the literature for conduction/radiation problems for cylindrical geometry. This note is concerned with the theoretical investigation of coupled conduction and radiation heat transfer in an absorbing, emitting, and anisotropically scattering gray medium bounded between two concentric cylindrical surfaces. The energy equation is solved by a finite difference method and the radiation transfer equation is solved by the discrete ordinates method (DOM) in conjunction with the Crank–Nicolson marching scheme. The effects of various parameters like emittance, scattering albdeo, scattering phase functions, conduction–radiation number, etc., on total heat flux are presented. For the case of isotropic scattering and diffusely reflecting walls, the results were also checked against those reported in literature[3] and are found to be in good agreement.

Mathematical Model

Consideration is given to steady-state, one-dimensional combined conduction and radiation heat transfer in an absorbing, emitting, and anisotropically scattering medium bounded between two concentric cylinders of inner and outer radii r_1 and r_2, respectively. The boundary surfaces reflect radiation both diffusely and specularly. It is assumed that the medium is gray; the boundary surfaces are gray, opaque, and isothermal; and the radiation intensity does not vary along the axis of the annulus. The thermal conductivity of the medium varies linearly with temperature as $k = k_0[1 + \alpha(T - T_1)]$. The energy equation for the medium may be written in dimensionless form as[5–7]

$$\frac{d^2\theta(\tau)}{d\tau^2} + \frac{1}{\tau}\frac{d\theta(\tau)}{d\tau} + \frac{\nu}{N_c + \nu[\theta(\tau) - 1]}\left[\frac{d\theta(\tau)}{d\tau}\right]^2 = \frac{(1 - \omega)}{N_c + \nu[\theta(\tau) - 1]}[\theta^4(\tau) - g(\tau)] \tag{1}$$

subject to the boundary conditions

$$\theta = 1 \quad \text{at} \quad \tau = \tau_1, \qquad \theta = \theta_2 \quad \text{at} \quad \tau = \tau_2 \tag{2}$$

where $g(\tau)$ is the dimensionless incident radiation function evaluated from the intensity distribution $I(\tau, \hat{s})$ as

$$g(\tau) = \frac{1}{4\sigma T_1^4}\int_{4\pi} I(\tau, \hat{s})\, d\Omega \tag{3}$$

$I(\tau, \hat{s})$ is evaluated from the solution of radiation transfer equation (RTE) together with the boundary conditions that are given next:

$$\mu\frac{\partial I(\tau, \hat{s})}{\partial \tau} + \frac{\eta}{\tau}\frac{\partial I(\tau, \hat{s})}{\partial \psi} + I(\tau, \hat{s}) = (1 - \omega)I_b(T) + \frac{\omega}{4\pi}\int_{4\pi} I(\tau, \hat{s}')p(\hat{s}, \hat{s}')\, d\Omega' \tag{4}$$

$$I(\tau_1, \hat{s}) = \varepsilon_1 I_b(T_1) + \frac{\rho_1^d}{\pi}\int_{\hat{n}_1\cdot\hat{s}'<0} I(\tau_1, \hat{s}')|\hat{n}_1\cdot\hat{s}'|\, d\Omega' + \rho_1^s I(\tau_1, \hat{s}_s) \tag{5}$$

$$I(\tau_2, \hat{s}) = \varepsilon_2 I_b(T_2) + \frac{\rho_2^d}{\pi}\int_{\hat{n}_2\cdot\hat{s}'<0} I(\tau_2, \hat{s}')|\hat{n}_2\cdot\hat{s}'|\, d\Omega' + \rho_2^s I(\tau_2, \hat{s}_s) \tag{6}$$

The total heat flux q, which is the sum of the conduction and the radiation contributions, may be obtained as

$$q(\tau) = -k\beta T_1\frac{d\theta(\tau)}{d\tau} + \int_{4\pi} I(\tau, \hat{s})\hat{n}\cdot\hat{s}\, d\Omega \tag{7}$$

Numerical Scheme

To obtain the temperature and the radiation intensity distributions, the energy equation Eq. (1) and the RTE Eq. (4) are to be solved simultaneously. A numerical iterative procedure is adopted for the solution. First a temperature distribution $\theta(\tau)$ is assumed, the RTE is solved to obtain the $I(\tau, \hat{s})$ distribution, the $g(\tau)$ profile is evaluated from Eq. (3), and then the energy equation is solved. The derivatives in the energy equation are replaced by second-order finite differences and this leads to a system of nonlinear algebraic equations with the nodal temperatures as the unknowns. This is solved by the Newton–Raphson method. RTE is solved by the discrete ordinates method (DOM)[6]. DOM converts the integrodifferential equation and the boundary conditions, Eqs. (4–6), into a two-point boundary-value problem in ordinary differential equations that are solved by a variant of the shooting method em-

Table 1 Comparison of $q(\tau_1)/k\beta T_1$ for the case of isotropic scattering and diffusely reflecting walls[a]

	$q(\tau_1)/k\beta T_1$					
	$N_c = 0.5$		$N_c = 0.1$		$N_c = 0.05$	
ω	Reference 3	Present work	Reference 3	Present work	Reference 3	Present work
			$\varepsilon_1 = \varepsilon_2 = 0.1$			
0	1.426	1.425	1.921	1.915	2.500	2.490
0.5	1.387	1.387	1.738	1.737	2.164	2.161
1	1.329	1.332	1.454	1.467	1.608	1.635
			$\varepsilon_1 = \varepsilon_2 = 0.5$			
0	1.523	1.522	2.430	2.429	3.566	3.565
0.5	1.498	1.498	2.308	2.309	3.330	3.334
1	1.468	1.470	2.148	2.155	2.998	3.012
			$\varepsilon_1 = \varepsilon_2 = 1$			
0	1.660	1.661	3.144	3.148	5.019	5.037
0.5	1.653	1.654	3.088	3.096	4.907	4.925
1	1.649	1.651	3.053	3.061	4.808	4.824

[a] $\tau_2 - \tau_1 = 1.0$, $r_1/r_2 = 0.5$, $\theta_2 = 0.1$, $\nu = 0.0$.

ploying the Crank–Nicolson scheme as the core integrator.[8] Numerical experience indicates that for low values of optical thickness, the numerical procedure for the RTE solution becomes unstable. However introduction of damping in the iterative scheme successfully overcame instabilities and produced converged solution. The whole numerical procedure is repeated until convergence, i.e., the maximum norm of the relative difference of the intensity and temperature distributions between two successive iterations falls below 1.0E-4.

Results and Discussion

To investigate the effect of anisotropic scattering in heat transfer we consider a linear anisotropic scattering (LAS) model. The single-scattering phase functions, $p(\mu_p)$, for the LAS model for various cases are given next, where μ_p is the cosine of the angle between the in-scattering and out-scattering directions.

Isotropic scattering:

$$p(\mu_p) = 1$$

Forward linear anisotropic scattering:

$$p(\mu_p) = 1 + \mu_p$$

Backward linear anisotropic scattering:

$$p(\mu_p) = 1 - \mu_p$$

The phase function $p(\hat{s}, \hat{s}')$ required in Eq. (4) can be easily obtained from $p(\mu_p)$.[9] The results discussed in this paper are based on the application of the S_8 method. All of the computations were carried out on an IBM-PC/AT-386 in single-precision arithmetic. Table 1 presents a comparison of the results obtained with the present analysis with that of Fernandes and Francis[3] for the case of isotropic scattering, diffusely reflecting boundaries, and without the effect of variable thermal conductivity. It may be seen that very good agreement exists between the present results and that of the previously mentioned reference.

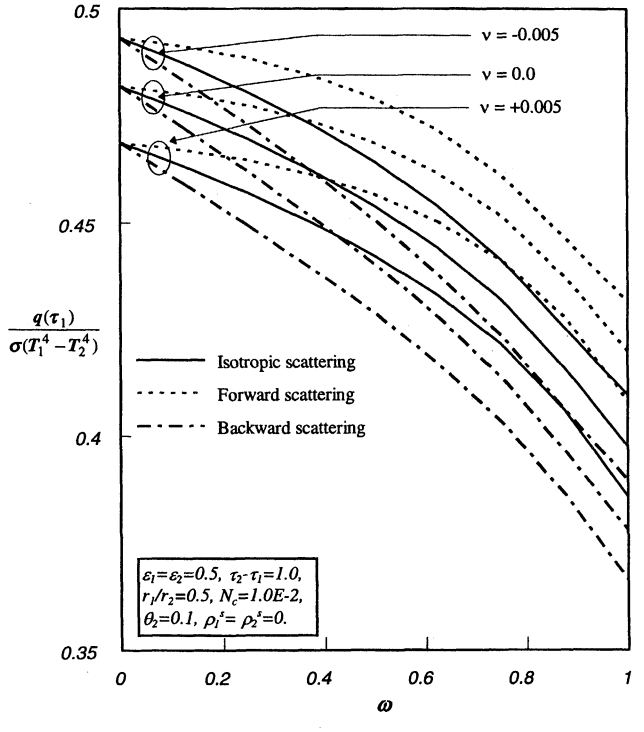

Fig. 1 Variation of heat flux with scattering albedo.

Figures 1–3 depict the heat flux results as a function of ω for different scattering phase functions and for various values of N_c and optical thickness. It is observed that the heat flux decreases with increasing ω for all the three phase functions. As N_c increases, the heat flux also increases, whereas for decreasing optical thickness the heat flux increases. An interesting observation was that, at very low values of N_c (of the magnitude of 1E-6), the heat flux increases with ω for isotropic and forward scattering, contrary to what was observed at high values of N_c. In all of the cases strongly backward scattering

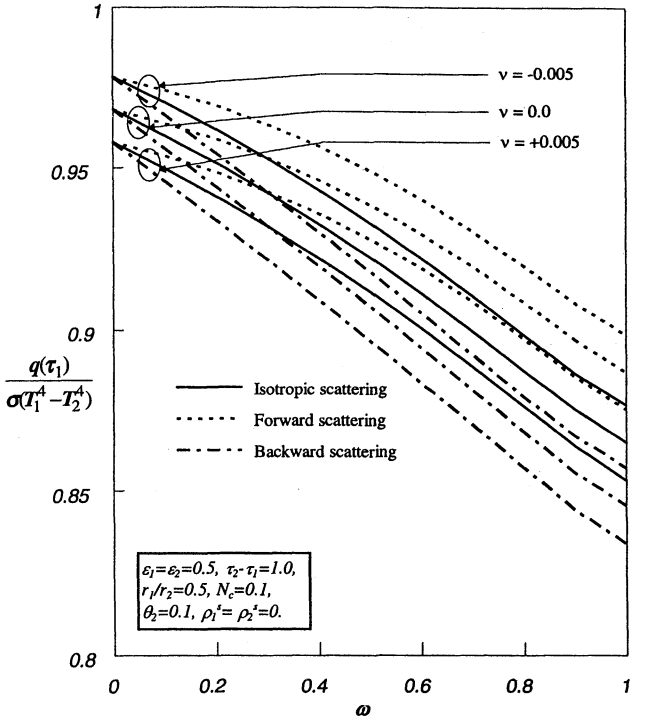

Fig. 2 Variation of heat flux with scattering albedo.

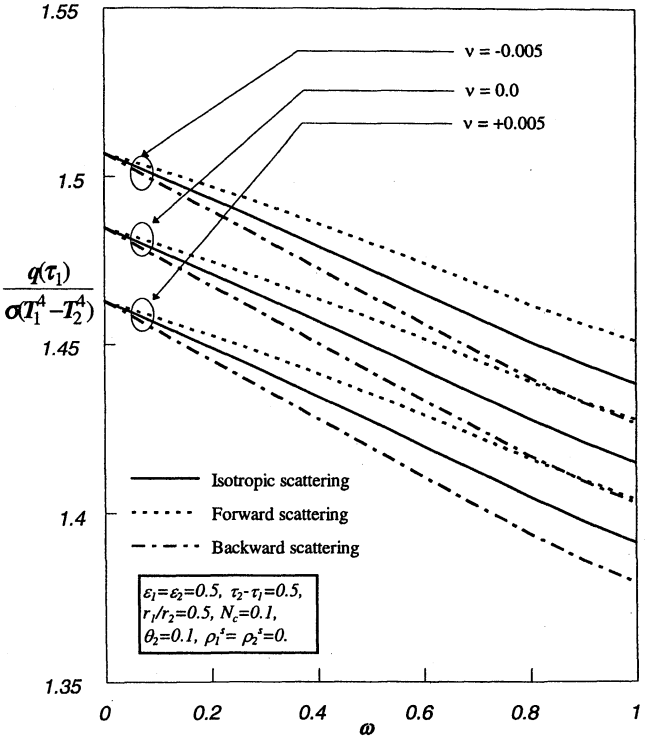

Fig. 3 Variation of heat flux with scattering albedo.

Table 2 Effect of specular reflection on heat flux[a]

		Dimensionless heat flux $q(\tau_1)/\sigma(T_1^4 - T_2^4)$					
		Isotropic scattering		Forward scattering		Backward scattering	
N_c	ω	Diffuse[b]	Specular[c]	Diffuse	Specular	Diffuse	Specular
0.001	0.1	0.0729	0.0709	0.0730	0.0710	0.0728	0.0708
	0.4	0.0662	0.0647	0.0666	0.0650	0.0659	0.0644
	0.9	0.0423	0.0420	0.0425	0.0422	0.0421	0.0418
	1	0.0255	0.0255	0.0255	0.0255	0.0255	0.0255
0.01	0.1	0.1967	0.1902	0.1972	0.1906	0.1962	0.1898
	0.4	0.1717	0.1676	0.1729	0.1688	0.1704	0.1664
	0.9	0.0985	0.0980	0.0989	0.0985	0.0980	0.0976
	1	0.0722	0.0722	0.0722	0.0722	0.0722	0.0722
0.1	0.1	0.7189	0.7071	0.7199	0.7080	0.7179	0.7062
	0.4	0.6739	0.6669	0.6765	0.6691	0.6715	0.6646
	0.9	0.5674	0.5669	0.5680	0.5674	0.5669	0.5664
	1	0.5397	0.5397	0.5397	0.5397	0.5397	0.5397

[a] $\varepsilon_1 = \varepsilon_2 = 0.03$, $\tau_2 - \tau_1 = 1.0$, $r_1/r_2 = 0.5$, $\theta_2 = 0.1$, $\nu = 0.0$. [b] $\rho^s = 0$, $\rho^d = \rho$. [c] $\rho^d = 0$, $\rho^s = \rho$.

displayed the lowest heat flux results. This observation is useful in selecting filler materials for multilayer insulations for cryogenic and space applications. It is interesting to note from Table 2 that fully specularly reflecting ($\rho^d = 0$, $\rho^s = \rho$) boundaries always transfer less heat than fully diffusely reflecting ($\rho^s = 0$, $\rho^d = \rho$) boundaries. This difference diminishes as ω and N_c increase. However, diffuse and specular results do not show any appreciable deviation. The effect of variable thermal conductivity is also shown in Figs. 1–3. For the case of thermal conductivity increasing with temperature, the heat transfer rate is less as compared to the opposite case. However, at lower values of N_c, the effect of variable conductivity diminishes slightly as ω increases.

Conclusions

1) The effect of anisotropy is significant, particularly for the case of low conduction–radiation numbers and high values of scattering albedo. At all values of conduction–radiation numbers, strongly backward-scattering media transfers the least heat and also affects a reducing heat transfer with increasing scattering albedo.

2) Specular or diffuse boundaries make little difference in heat transfer, although the former transfer less heat.

3) The effect of variable thermal conductivity is significant.

Acknowledgments

The author acknowledges K. Badari Narayana, Head Thermal Design Section; D. R. Bhandari, Head, Thermal Design and Analysis Division; H. Narayanamurthy, Group Director, Thermal Systems Group; and A. V. Patki, Deputy Director, ISRO Satellite Centre, for their support and encouragement during the course of this work.

References

[1]Viskanta, R., "Radiation Transfer: Interaction with Conduction and Convection and Approximate Methods in Radiation," *Proceedings of the 7th International Heat Transfer Conference* (Munich, Germany), Vol. 1, 1982, pp. 103–121.

[2]Howell, J. R., "Thermal Radiation in Participating Media: The Past, the Present, and Some Possible Futures," *Journal of Heat Transfer*, Vol. 110, 1988, pp. 1220–1229.

[3]Fernandes, R., and Francis, J., "Combined Conductive and Radiative Heat Transfer in and Absorbing, Emitting, and Scattering Cylindrical Medium," *Journal of Heat Transfer*, Vol. 104, 1982, pp. 594–601.

[4]Pandey, D. K., "Combined Conduction and Radiation Heat Transfer in Concentric Cylindrical Media," *Journal of Thermophysics and Heat Transfer*, Vol. 3, No. 1, 1989, pp. 75–82.

[5]Harris, J. A., "Solution of the Conduction/Radiation Problem with Linear-Anisotropic Scattering in an Annular Medium by the Spherical Harmonics Method," *Journal of Heat Transfer*, Vol 111, 1989, pp. 194–197.

[6]Modest, M. F., *Radiative Heat Transfer*, McGraw–Hill, New York, 1993.

[7]Chu, H. S., and Tseng, C. J., "Conduction-Radiation Interaction in Absorbing, Emitting and Anisotropically Scattering Media with Variable Thermal Conductivity," *Journal of Thermophysics and Heat Transfer*, Vol. 6, No. 3, 1992, pp. 537–540.

[8]Hall, G., and Watt, J. M. (ed.), *Modern Numerical Methods for Ordinary Differential Equations*, Clarendon, Oxford, England, UK, 1976.

[9]Brewster, M. Q., *Thermal Radiative Transfer and Properties*, Wiley, New York, 1992.

Air High-Enthalpy Stagnation Point Heat Flux Calculation

F. De Filippis* and M. Serpico†
Centro Italiano Ricerche Aerospaziali,
Via Maiorise 81043 Capua, Italy

Introduction

A SPACE vehicle re-entering into the atmosphere is subject to very high thermal loads, because of the conduction and diffusion of energy through the boundary layer and, naturally, the stagnation region is the more stressed zone. Since 1950, hypersonic researchers have made great efforts to find analytical formulas to evaluate the heat-flux peak at the stagnation point. The theory developed by Fay and Riddell[1] in 1958 represents the most important milestone in this field. In their work Fay and Riddell solve the self-similar boundary-layer equations, taking into account the main chemical–physical effects in the air at high enthalpy (in particular dissociation and diffusion) for equilibrium or frozen boundary layer. The limited computer resources in 1958 imposed a great number of approximations. The viscosity and the thermal conductivity were modeled using the Sutherland law extrapolation at high temperature; the diffusivity was modeled assuming a constant value of the Prandtl number and considering the air mixture composed of only two species: molecular and atomic types. The final formulas proposed by Fay and Riddell, that are still in use today, permit the evaluation of the stagnation point heat flux starting from the flow properties at the external boundary-

Received April 7, 1997; revision received May 11, 1998; accepted for publication May 28, 1998.

*Research Scientist, Plasma Wind Tunnel Section. Member AIAA.
†Ph.D., Research Engineer, Aerothermodynamics Section.